AAS 25-240

STRATEGIES AND APPLICATIONS FOR SUSTAINED MULTI-VEHICLE LOITERING IN THE GATEWAY NRHO

Brian McCarthy*, Stephen Scheuerle†, Emily Zimovan-Spreen‡, and Diane Davis§

The lunar Gateway plans to operate in an L_2 Near Rectilinear Halo Orbit (NRHO) near the Moon for nominal operations. During the mission's lifetime, various visiting vehicles may need to loiter on an alternate trajectory for a considerable amount of time. This investigation examines various strategies and configurations for visiting vehciles loitering near the Gateway. Characteristics of loitering in a string of pearls or quasi-periodic orbit configuration in the ephemeris model are investigated with consideration of operational errors. For sustained loitering in the NRHO, modifications to orbit maintenance strategies are discussed. Additionally, variations from predicted baseline trajectories are examined to understand the impacts for an as-flown spacecraft.

INTRODUCTION

In November 2022, the Artemis I mission launched an uncrewed Orion capsule to test the first component of the campaign to develop a sustained human presence in cislunar space.[1] One aspect of this campaign is the development of the lunar Gateway station, which will serve as a testbed for humans to live and work in deep space. The Gateway plans to operate in a southern Earth-Moon L_2 Near Rectilinear Halo Orbit (NRHO) in a 9:2 resonance with the lunar synodic period. Given that the Gateway plans to serve as a hub between Earth, the lunar surface, and other locations in deep space, visiting vehicles will be a consistent presence in the vicinity of the Gateway. Consequently, a characterization of the regions where visiting vehicles can remain to keep a safe distance from the Gateway is required. The Gateway NRHO exists in a unique multi-body dynamical environment, where the gravitational effect of the Earth and Moon are necessary to describe the motion. One objective of this investigation is to assess safe loitering regions in the vicinity of the Gateway's NRHO. Understanding safe regions in the vicinity of the NRHO can help inform visiting vehicle mission profiles as well as provide a guideline for vehicles operating near Gateway. Several comparisons are considered in this investigation to understand how individual baseline NRHO trajectories vary as well as how variations between vehicles maintained in their respective baselines behave.

Several previous investigations have examined relative motion, rephasing, and loitering trajectories in the vicinity of NRHOs. Khoury and Howell examined loitering applications in the vicinity of a 9:2 NRHO in the Circular Restricted Three-Body Problem (CR3BP).[2] Sandel and Sood examined

*Gateway Mission Design Engineer, a.i. solutions, Inc., 2101 E NASA Pkwy, Houston, TX 77058; brian.p.mccarthy@nasa.gov
†Gateway Mission Design Engineer, NASA JSC, 2101 E NASA Pkwy, Houston, TX 77058; stephen.t.scheuerle@nasa.gov
‡Gateway Mission Design Deputy Lead, NASA JSC, 2101 E NASA Pkwy, Houston, TX 77058; emily.m.spreen@nasa.gov
§Gateway Mission Design Lead, NASA JSC, 2101 E NASA Pkwy, Houston, TX 77058; diane.c.davis@nasa.gov

proximity operations and rendezvous for a low-thrust spacecraft in an NRHO.[3] Additionally, Davis et al. examined a process to shift the phase within a 9:2 NRHO using the nominal Gateway stationkeeping algorithm in an ephemeris model.[4] Rendezvous design was also examined by Blazquez et al. in an ephemeris model.[5] Bucchioni et al. examined different phasing orbit configurations and leveraged manifold trajectories for cargo vehicles in the vicinity of the 9:2 NRHO in the CR3BP.[6] More recently, McCarthy et al. examined leveraging two-burn and four-burn transfers to rephase in the vicinity of the Gateway's NRHO.[7] Nugent et al. as well as Nugent and Howell examined strategies for short-term loitering using stretching and stability information.[8,9]

First, a summary of differences between NRHO baselines constructed using a process developed by Zimovan-Spreen et al. is presented examining various phases along the Gateway baseline NRHO.[10] Next, previous work by Davis et al. is extended to further investigate variations between a stationkept Gateway and the long-term baseline NRHO trajectory.[11] Different stationkeeping strategies are investigated with the goal of maintaining the spacecraft closer to its baseline trajectory. Crewed and uncrewed configurations of the Gateway are introduced to understand how different strategies are affected by varying levels of perturbations. Additionally, the behavior of a predicted Gateway spacecraft ephemeris is examined. Then, differences between stationkept vehicles in various phases of the 9:2 NRHO are examined to understand how loitering vehicles behave relative to each other. The results of this investigation provide a clearer picture of the safe loitering regions around the Gateway.

DYNAMICAL MODELS

Two dynamical models are leveraged in this investigation, the Circular Restricted Three-Body Problem (CR3BP) and a higher-fidelity ephemeris model. The CR3BP offers higher fidelity and additional behaviors in comparison to the two-body model. In this model, two gravitational bodies, denoted P_1 and P_2, remain in circular Keplerian orbits about their mutual barycenter (i.e., center of mass). A third body, P_3, moves under the gravitational influence of the two larger bodies and is assumed to be massless. The model is defined relative to a rotating coordinate system, where the $+\hat{x}$ direction is defined from the barycenter toward P_2. The $+\hat{z}$ direction is defined parallel to the direction of the orbital angular momentum vector for P_1 and P_2; the $\hat{y}$ direction completes the orthonormal triad. The position and velocity of P_3 relative to the barycenter in the rotating frame are defined as $\vec{x} = \begin{bmatrix} x & y & z & \dot{x} & \dot{y} & \dot{z} \end{bmatrix}^T$, where the first three and the last three elements are the position and relative velocity components, respectively. The equations of motion for a particle moving in the CR3BP are a set of three, second-order scalar differential equations of motion,

$$\ddot{x} - 2\dot{y} = \frac{\partial U^*}{\partial x} \qquad \ddot{y} + 2\dot{x} = \frac{\partial U^*}{\partial y} \qquad \ddot{z} = \frac{\partial U^*}{\partial z} \tag{1}$$

The pseudo-potential is a scalar defined solely as a function of position and the CR3BP mass parameter, $\mu = M_2/(M_1 + M_2)$, where M_1 and M_2 are the masses of P_1 and P_2, respectively.[12] The pseudo-potential function takes the following form,

$$U^* = \frac{x^2 + y^2}{2} + \frac{\mu}{r} + \frac{1-\mu}{d} \tag{2}$$

where $d = \sqrt{(x+\mu)^2 + y^2 + z^2}$ and $r = \sqrt{(x-1+\mu)^2 + y^2 + z^2}$ represent the distances of P_3 relative to P_1 and P_2, respectively. The CR3BP admits a single integral of the motion, commonly

denoted the Jacobi Constant (JC). The Jacobi Constant is a function of the pseudo-potential and the relative velocity magnitude expressed in the rotating reference frame,

$$JC = 2U^* - v^2 \tag{3}$$

where $v = \sqrt{\dot{x}^2 + \dot{y}^2 + \dot{z}^2}$. The Jacobi Constant is an energy-like quantity that characterizes motion in a CR3BP system and remains constant for all time over any ballistic arc propagated in the CR3BP. One advantage of the CR3BP model is that the system is time invariant, which is important for examining trajectories independent of epoch. The CR3BP is also a good approximation for a multi-body environment and the trajectory characteristics generally persist when transitioning results to a higher-fidelity ephemeris model.

The ephemeris force model offers a higher-fidelity gravity force representation on the spacecraft by incorporating the ephemeris states of various celestial bodies. The interpolated position and velocity state corresponding to these bodies are extracted from the ephemerides on the JPL NAIF server.[13] The analysis performed in the ephemeris model reinforces the result found in the CR3BP and represents a more realistic cislunar environment to execute a scenario during an Artemis mission. The specific ephemeris model leveraged in this investigation is summarized by Zimovan-Spreen et al.[10] In this analysis, the term "baseline" denotes a long-term trajectory used to define orbit maintenance targets for each spacecraft. The baseline roughly represents the expected path of the spacecraft. Because the orbit maintenance algorithm planned for use in the NRHO ensures a spacecraft remains near the planned NRHO, but not precisely on the trajectory, the term "baseline" is selected in place of the term "reference".

NRHO TRAFFIC MANAGEMENT

NRHO traffic management is critical to ensure safety for visiting vehicles throughout the Artemis campaign and beyond. The complex cislunar dynamics and specific vehicle requirements introduce challenges for trajectory design in the cislunar region. Driven by the Artemis mission concept of operations and requirements, relative motion for vehicles in the 9:2 NRHO is classified into four regimes. These regimes are denoted long-term loitering, medium-term loitering, short-term loitering and port relocation. The specifics of each of these loitering regimes are defined as follows:

- **Long-term loitering** considers two separate vehicles operating in and maintaining the underlying 9:2 NRHO. Vehicles in a long-term loiter are not planned to rendezvous and dock with Gateway. For example, consider Gateway and a robotic satellite carrying out a science mission. The satellite may be stationed in a long-term loiter in a different phase of the 9:2 NRHO or another NRHO in the vicinity. Although the two vehicles reside in the same orbit, there is no nominal intent to encroach on one another.

- **Medium-term Loitering** considers two or more vehicles operating in the 9:2 NRHO, leading up to an rendezvous and docking event within 90 days. Medium-term loitering comprises multiple revolutions of the 9:2 NRHO where each vehicle individually maintains its respective trajectory prior to an approach to Gateway. For example, consider Gateway and a single visiting vehicle. The visiting vehicle may transfer into the 9:2 NRHO, where it will operate for several revolutions prior to rendezvous and docking. During this period, Gateway and the visiting vehicle independently perform maneuvers to maintain their respective orbits/phases. The significant difference between long-term and medium-loitering is that the loitering vehicle(s) remain near Gateway and intend to dock to Gateway after the medium-term loiter.

Thus, the drivers for design of a medium-term loiter concept of operations requires a balance between vehicle safety and overall propellant usage for the transfer from the loiter location to Gateway.

- **Short-term Loitering** considers two vehicles loitering near each other for less than one revolution of the NRHO (< 6.5 days). Short-term loitering is planned prior to a docking sequence or immediately after undocking. An example of short-term loitering is a visiting vehicle's trajectory prior docking with Gateway. The visiting vehicle may loiter near Gateway for several hours or days while other vehicles dock, relocate, or undock. During this period, the visiting vehicle must ensure a safe trajectory to avoid inadvertent conjunctions with Gateway or other visiting vehicles. The investigation by Scheuerle et al. addresses strategies for short-term loitering near Gateway.[14]

- **Port relocation** considers a visiting vehicle as it relocates from one docking port to another over the course of several hours. An example of a port relocation is a visiting vehicle that delivers a new module to Gateway. The visiting vehicle may first dock and deliver the module to one docking port, proceed to undock, and relocate to another docking port. The nominal amount of time undocked from Gateway is a few hours, where the vehicles operate in near proximity as one maneuvers to the proper orientation.

The analysis in this investigation focuses on the dynamics and strategies for medium-term loitering near Gateway.

LOITERING CONFIGURATIONS

Formation flying has been successfully executed for operations on the International Space Station (ISS) for many vehicles. The formation flying strategies for the ISS rely on the assumption that the orbit is nearly conic; however, given that the Gateway will operate in a more complex dynamical environment, the two-body assumption is no longer valid.[15,16] Therefore, it is useful to leverage dynamical structures of a multi-body model, given that the NRHO is a three-body orbit, to help design trajectories that remain near the Gateway NRHO. Two loiter/relative motion configurations are considered in this investigation: string of pearls and quasi-periodic orbits.

String of Pearls Loitering

While the Gateway plans to operate in a certain eclipse-favorable NRHO phase, visiting vehicles may also be loitering "ahead" or "behind" the Gateway. This configuration of loitering is defined as string of pearls, where the vehicles follow the same path but are phased at different locations around the orbit. Altering the amount of time "ahead" or "behind" a deputy spacecraft loiters relative to the chief changes the close approach distance. The phasing time is defined as the separation time between the deputy and the chief. If the chief passes over perilune before the deputy, then the deputy is considered to be "behind," while a deputy that passes perilune prior to the chief is "ahead." Since the orbital speed is slower near apolune, the minimum distances between spacecraft occur when the deputy and chief are close to apolune. In the Earth-Moon CR3BP, the 9:2 NRHO is periodic, i.e., the time between successive periapsis points remains constant ($\sim$6.56 days). Given the periodic nature of the 9:2 NRHO in the CR3BP, initial phasing in a string of pearls configuration is examined first in the simplified model. In Figure 1, the minimum distance between the deputy and chief is plotted as a function of the phasing time along the NRHO. In Figure 1(a), the close approach distance is plotted

for separation times up to half an NRHO revolution. At a 3-day separation time, the spacecraft never pass closer than 24,900 km. A zoomed-in view for separation times up to 5 hours appears in Figure 1(b). With a 1-hour separation, the close approach distance is 374 km.

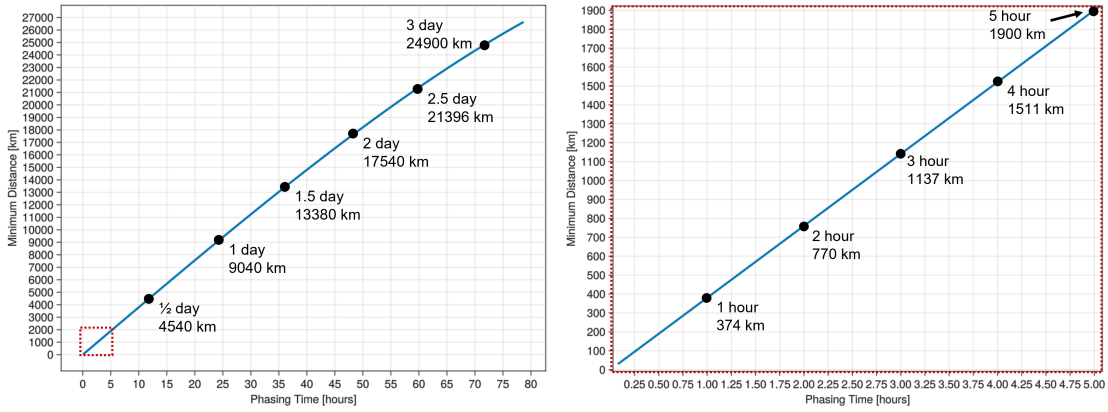

(a) (b)

Figure 1. Using a string of pearls configuration in the NRHO, the minimum distance between the deputy and chief is plotted as a function of the phasing time in the CR3BP for a (a) half period of the orbit in phasing time and (b) zoomed into the area from zero to 5 hours of phasing time.

Quasi-Periodic Orbit Loitering

In addition to a string of pearls configuration, quasi-periodic orbits provide an alternate type of configuration for loitering near the 9:2 NRHO. Instead of loitering "ahead" or "behind", quasi-periodic orbits (QPOs) "twist" around the periodic 9:2 NRHO. These types of orbits have been studied by several previous researchers for relative motion trajectory design applications in multi-body environments.[17–21] QPOs exist in families that emanate from certain periodic orbits and possess characteristics that allow the motion to stay bounded nearby a spacecraft in a periodic NRHO.[18,22] Additionally, this class of orbit is known to exist in a higher-fidelity ephemeris model and transition methods exist to ensure they maintain their characteristics after the transition.[18,23] Surfaces representing fixed longitudinal period quasi-periodic 9:2 NRHOs appear in Figure 2(a), and a specific trajectory that exists on one of the surfaces appears in Figure 2(b). The fixed longitudinal period QPO family possesses the same longitudinal period as the 9:2 NRHO, such that, over time, a trajectory on the quasi-periodic orbit does not drift out of phase with the periodic 9:2 NRHO. Consider the phasing time difference of the two trajectories. The phasing time is the difference between the perilune passage time of the underlying periodic NRHO and the perilune passage time of the quasi-periodic NRHO. The phasing time for several revolutions of the QPO loitering case and the underlying NRHO is presented in Figure 2(c). The phasing time difference per revolution of the orbit is calculated for the quasi-periodic loitering case and plotted in Figure 2(c) using the trajectory from Figure 2(b). Unlike the string of pearls configuration, the phasing time does not remain constant but oscillates from revolution to revolution, with an amplitude of approximately 2.5 hours.

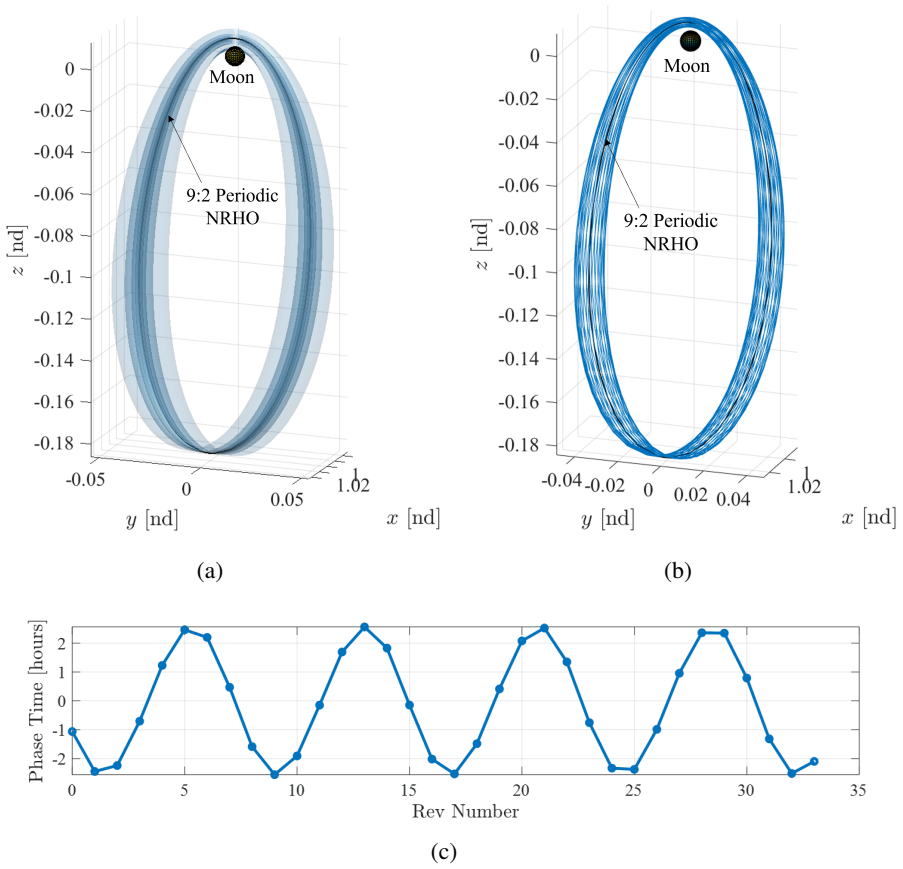

Figure 2. (a) The periodic 9:2 NRHO (black) and several members of the fixed longitudinal period family (blue surfaces) of quasi-NRHOs in the CR3BP. (b) Quasi-NRHO trajectory propagated for 34 revs (blue) and the periodic 9:2 NRHO (black). (c) Phasing time of the quasi-NRHO trajectory from (b) relative to the periodic 9:2 NRHO.

NRHO BASELINES

Currently, the Gateway orbit maintenance strategy leverages a long-term, continuous baseline trajectory that spans the lifetime of the mission. The construction of these baseline trajectories in an ephemeris model is performed using a multiple shooting technique summarized by Zimovan-Spreen, et al.[10] The Gateway baseline NRHO is specifically phased such that long-duration eclipses are avoided. There are some additional characteristics of this orbit that are affected by the perigee-syzygy period of the Sun-Earth-Moon system. The perigee-syzygy occurs approximately every 413 days, or every 14 synodic months, when the Sun, Earth and Moon are aligned and the Moon is located at its perigee. This 413-day period is observed in the NRHO baseline trajectory in Figure 3(a), where a periapsis Poincaré map is represented using the $\hat{x}\hat{y}$-components of the position in the Earth-Moon rotating frame. The points in Figure 3(a) are the periapses associated with a 20-year eclipse-favorable NRHO baseline trajectory in the ephemeris model and colored by a index number 1 through 9. Each index corresponds to a specific Sun-Earth-Moon geometry in the 9:2 synodic resonance of the NRHO. For each index number, there are 7 groupings of points, as highlighted in Figure 3(b) using index 5, colored in purple. Thus for every 63, i.e., 9×7, revolutions of the NRHO,

the trajectory returns to one of these groupings of points. This repetitive 63-revolution behavior is related to the perigee-syzygy period, in that 63 revolutions of the NRHO is approximately equal to 413 days or 14 synodic months. This phenomenon also exists for the alternate eclipse-favorable phase of the 9:2 NRHO.[10]

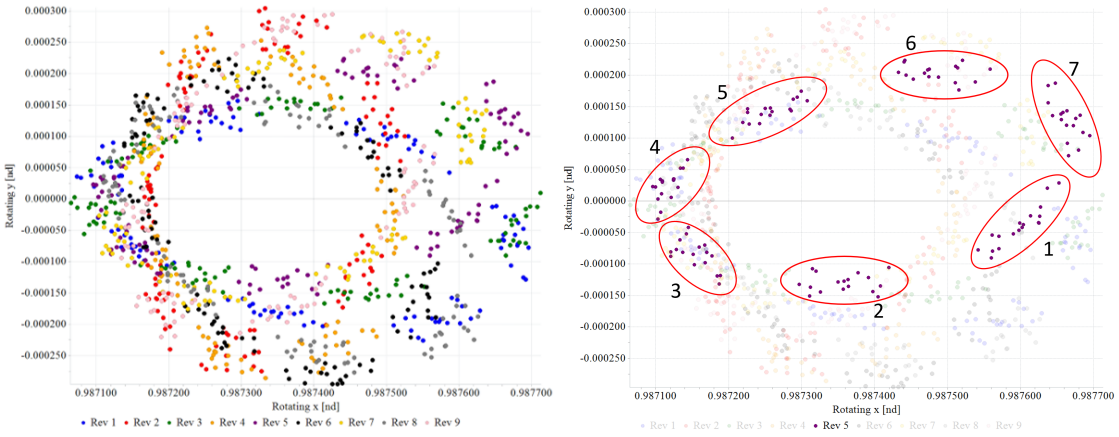

(a) (b)

Figure 3. (a) Periapsis points along the 20-year NRHO baseline trajectory, projected in the $\hat{x}\hat{y}$-plane of the Earth-Moon rotating frame. (b) Highlighted periapsis points for every 5th revolution of the 20-year NRHO baseline trajectory.

The time between perilune passes varies with each revolution of the NRHO baseline in the higher fidelity ephemeris model. It is useful to understand variations in the orbital period for a single NRHO baseline as well as how the phasing between two different baselines varies. To validate the results computed in the CR3BP in Figure 1, several two-year long baseline NRHO trajectories are generated at various phases. The same algorithm developed by Zimovan-Spreen et al. is leveraged to develop each baseline to ensure the phase offset remains consistent over time. In Figure 4, five phase-offset baselines are compared to a nominal 2-year baseline to ensure that the phasing difference remains consistent in the ephemeris model. In Figure 4(a), the minimum range between the phase-shifted NRHO (deputy) and the nominal NRHO (chief) is plotted as a function of the phase difference for each revolution. To ensure that the phasing does not drift over time, the phase difference between the phase-shifted baseline and nominal baseline is plotted as a function of the revolution number in Figure 4(b). Note that the minimum distance computed in Figure 4(a) is consistent with the results computed in the CR3BP in Figure 1(b). However, care must be taken in the construction of baselines to ensure consistent behavior. It is observed that baselines constructed with differing durations tend to drift relative to one another when generated using the methods described in Zimovan-Spreen et al. For example, consider the comparisons in Figure 5. In these plots, the phase offset baselines with 2-year durations are compared to a 20-year baseline constructed by Zimovan-Spreen et al. A drift in phase is observed in Figure 4. Note that over the 2-year period, the phase-shifted trajectories possess higher amplitude variations in phase difference. Also, the slight positive trend in Figure 5(a) demonstrates that the baselines are drifing in phase across the two-year time period. To help combat that drift and minimize the oscillations in phase, phase-shifted baselines are generated for the same 20-year duration and compared in Figure 5(b). The secular drift in the baselines is removed, as desired. However, observe in Figure 5(b), there exists a long-period oscillation, whose period is approximately equal to the Saros period, or roughly 18 years. This period also

distinguishes the two eclipse-favorable phases of the NRHO, as highlighted by Zimovan-Spreen et al.[24] For a string of pearls configuration, consistent phasing "ahead" or "behind" the chief baseline is critical for loitering vehicles to ensure that the deputy baseline does not eventually drift toward the chief baseline. In summary, to ensure that the oscillations and drift between phase shifted baselines are nulled as much as possible, generating baselines that have an equal duration is recommended when employing the generation method described by Zimovan-Spreen et al.

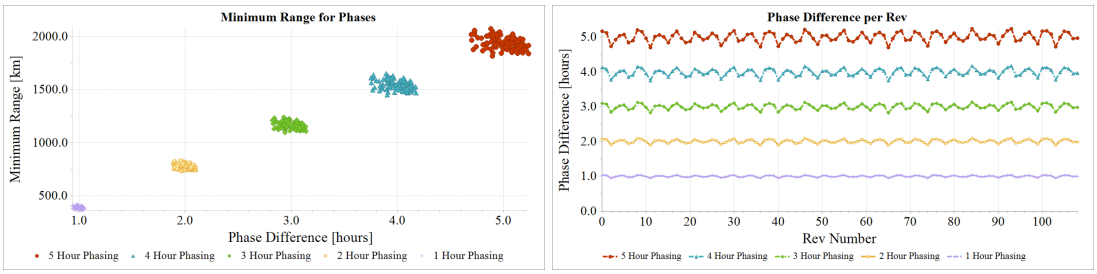

(a) (b)

Figure 4. (a) The minimum distance over various 2-year long baseline NRHOs is plotted as a function of the phase offset for that revolution. (b) The phase offset is plotted as a function of the revolution number.

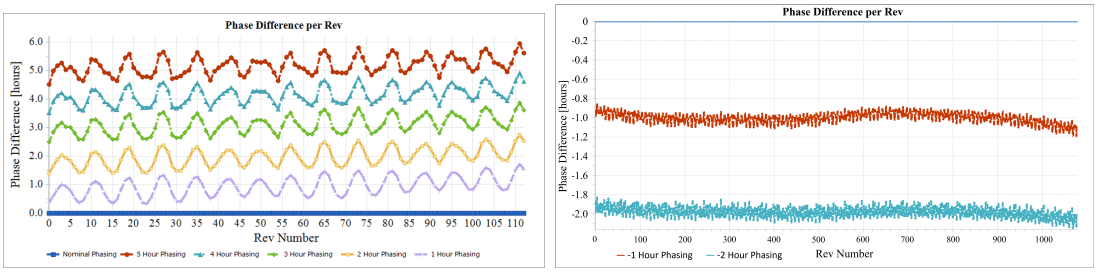

(a) (b)

Figure 5. (a) The phase offset of 2-year duration baselines is plotted as a function of the revolution number relative to the Phase A eclipse free baseline. (b) The phase offset is plotted as a function of the revolution number for 20-year baselines relative to the Phase A eclipse-free 20-year baseline.

As noted in the previous section, quasi-periodic orbits in the vicinity of Gateway offer another configuration for loitering vehicles to remain nearby by loitering in the vicinity or "twisting" around the Gateway's orbit. Quasi-periodic NRHOs have been examined in various models by several previous researchers.[18,25,26] Families of quasi-periodic orbits exist in a variety of multi-body models. To maintain the characteristics associated with the Sun-Earth-Moon dynamics, a transition process from a four-body model is used to generate long-term reference quasi-periodic baseline trajectories. The process is summarized by Brown et al., where trajectories along QPOs are transitioned from the Hill Restricted Four-Body Problem (HR4BP) to the Sun-Earth-Moon ephemeris model and are analyzed relative to their ephemeris-transitioned periodic orbit counterpart.[18] The derivation and assumptions associated with the model are summarized by Scheeres.[27] An example of an ephemeris-transitioned quasi-periodic orbit and the ephemeris-transitioned periodic orbit counterpart are rendered in the Earth-Moon rotating frame in Figure 6(b). The zoomed-in view near

perilune shows that the periodic orbit counterpart (white) appears to remain "inside" of the quasi-periodic orbit (red) in Figure 6(a). The red and white circles in Figure 6(a) represent the perilunes of the respective trajectories over each revolution of the Moon. By examining several quasi-periodic orbits that have various "widths" relative to the Gateway NRHO, the minimum distance and variations in phasing are assessed. In Figure 7(b), the phase offset at perilune is plotted as a function of the orbit revolution number. Note that the quasi-periodic NRHOs oscillate around the periodic NRHO with various amplitudes. Even though there are situations where the QPO phase is nearly zero relative to the periodic orbit, the trajectories often are not in the same position at a particular epoch. This phenomenon is highlighted in Figure 7(a), where the minimum distance between each of the ephemeris-transitioned QPOs relative to the ephemeris-transitioned periodic orbit is computed as a function of the phase difference. As is the case for the string of pearls configuration, the minimum distance occurs near apolune. The minimum distance is always greater than zero, i.e., the deputy trajectory remains nearby, but does not intersect the chief trajectory, assuming the quasi-periodic trajectory is phased properly.

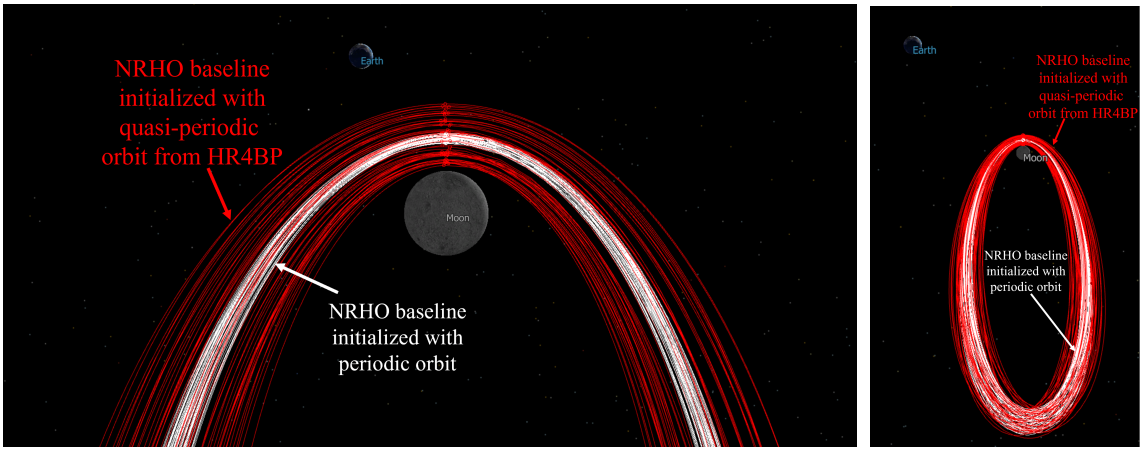

(a) (b)

Figure 6. (An ephemeris-transitioned QPO (red) and the underlying ephemeris-transitioned periodic orbit (white) in the Earth-Moon rotating frame (a) zoomed-in near near perilune and (b) a wider view of both orbits.

VARIATIONS BETWEEN BASELINE AND AS FLOWN SPACECRAFT

Characterizing motion in the baseline trajectories is useful for understanding the general behavior in the ephemeris model, but the baselines may not represent the as-flown trajectories of a vehicle. In the case of Gateway in particular, the orbit maintenance strategy is not designed to correct the trajectory tightly back to the baseline NRHO. Instead, information from the baseline NRHO is used to generate a catalog of orbit maintenance targets, and the strategy maintains the period, phase, and other orbit characteristics without using a target-point stationkeeping approach. Additionally, various errors and perturbations on the vehicle also dictate differences between the planned versus as-flown trajectory. These errors and perturbations must be considered for loitering vehicles as well to ensure that the as-flown loitering paths remain safe. First, an understanding of the variations of Gateway relative to its baseline trajectory are examined. Then, modifications to the orbit maintenance algorithm are performed to decrease deviations between the as-flown spacecraft and

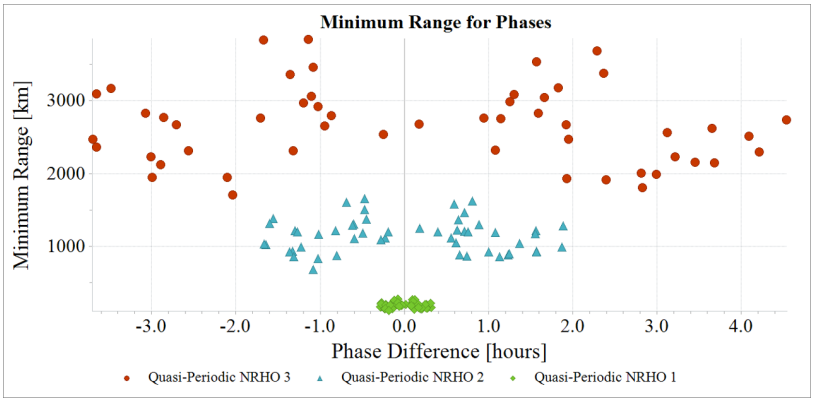

(a)

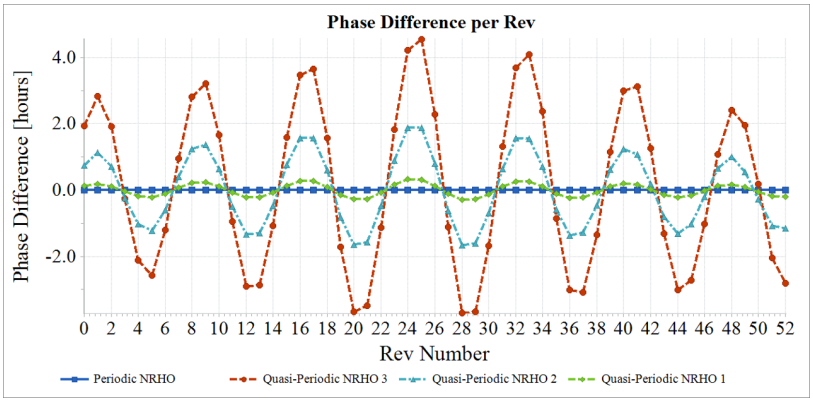

(b)

Figure 7. (a) The minimum distance of various ephemeris-transitioned quasi-periodic NRHOs compared to an ephemeris transitioned-periodic orbit is plotted as a function of the phase offset for each revolution. (b) The phase offset is plotted as a function of the revolution number.

the baseline trajectory. Lastly, the modifications are validated using the higher-fidelity Gateway Mission Design and Analysis Software (MiDAS) to ensure that the results remain consistent.

The Gateway leverages an orbit maintenance scheme that targets the rotating $\hat{x}$ component of velocity and the perilune passage time of an NRHO baseline trajectory at a perilune location 6+ revolutions downstream from where the orbit maintenance maneuver (OMM) is being executed. The location of OMM execution is defined at an osculating Moon-centered true anomaly of 200 degrees. Additional details of the algorithm are summarized by Davis et al.[28] The tuning of the orbit maintenance scheme is adjusted through several variables, including the tolerances applied to burn targeting. Nominally, the rotating v_x is targeted within +/- 0.45 m/s and the perilune passage time, t_p, is targeted within +/- 15 minutes of the values along the baseline trajectory. Given that the maneuvers are targeted 6 revolutions downstream and a weighting term is employed, the vehicle stays within +/- 50 minutes of perilune passage time relative to the baseline NRHO. The variations from the baseline when the vehicle performs OMMs under various navigation and maneuver execution errors as well as desaturation maneuvers are summarized by Davis et al.[11] Note that the maximum deviation is approximately 4500 km, which occurs near perilune where the vehicle is moving the fastest. While a maximum deviation of 4500 km might be acceptible for uncrewed Gateway opera-

tions, there may be scenarios where the vehicle needs to remain closer to the baseline NRHO, i.e. for rendezvous and docking of visiting vehicles, crewed operations, etc. To satisfy tighter constraints, the orbit maintenance algorithm can be modified to reduce variations from the baseline NRHO at an increased maneuver cost. Specifically, the targeting horizon time can be reduced, and the perilune passage time tolerance can be tightened to yield closer adherence to the NRHO baseline.

To understand the effects of varying each of the targeting parameters, combinations of t_p tolerance and targeting horizon time are used in a year-long stationkeeping simulation. The targeted horizon is varied from 2 to 6 revolutions downstream, and t_p tolerances of 15, 5, 1, 0.1, and 0.01 minutes are considered. Monte Carlo simulations are run using 100 trials for all combinations of t_p tolerances and horizon times. Errors included in the simulation are noted in Table 1.The desaturations are applied in random directions with magnitudes sampled from a zero-mean Gaussian distribution with a 3σ value of 1.0 cm/s. Insertion errors are applied to a state along the baseline NRHO at the beginning of each trial to set the initial condition of the spacecraft. Navigation errors are applied 24 hours before each OMM to simulate a tracking data cutoff. Maneuver execution errors are applied according to a Gates model, and SRP area and SRP coefficient errors are applied at the start of each NRHO revolution. The results are plotted in Figure 8 for all combinations of horizon times and t_p tolerances, showing the average maneuver cost per year, the standard deviation of the maneuver costs, and the maximum variation in the perilune passage time relative to the baseline NRHO. Note that the plot of perilune passage time variations in Figure 8(c) is rotated 180 degrees relative to Figures 8(a) and 8(b) and that the scale for t_p tolerance is a log scale. The red dot in the corner of each of the plots represents the metrics using the nominal OMM horizon time (6 revolutions ahead) and t_p tolerance (15 minutes). This nominal case has the lowest maneuver cost of all the simulations, as expected from previous analysis.[28] For all cases where the t_p tolerance is greater than or equal to 1 minute, the number of revolutions ahead does not have a significant effect on the perilune passage time variations relative to the baseline NRHO. However, the mean Δv and standard deviation of the Δv required to maintain the trajectory increases for shorter horizon times. Considering the nominal horizon time, i.e., 6 revolutions ahead, the minimum perilune passage time deltas occurs when the t_p tolerance is set at 1 minute, denoted by the orange dot in Figure 8. The perilune passage time variations begin to increase again when the t_p tolerance is reduced further.

The perilune passage time deltas are plotted in Figure 9 for a horizon of 6 revolutions for t_p tolerance values of 5, 1, and 0.1 minutes. In the plots in Figure 9, note that as the t_p tolerance is reduced, oscillations appear in the perilune passage time. Those oscillations also increase as time progresses. Also note that the scales on the y-axes are different between the plots in Figure 9. Given that the oscillations are not apparent and no secular growth is observed with a t_p tolerance of 5 minutes in Figure 9(a), but both oscillations and secular growth are present with a t_p tolerance of 1 minute in Figure 9(b), there exists a t_p tolerance between 1 and 5 minutes that minimizes the perilune passage time over a one year simulation for a 6 revolution horizon time. This oscillatory phenomenon has been identified by previous researchers and is damped by including an the rotating y-position component as a targeting parameter for OMMs.[4] However, inclusion of damping maneuvers requires more Δv for a given maneuver than a nominal OMM that only targets v_x and t_p tolerance. Thus, avoiding the oscillations with careful selection of targeting parameters is preferred.Lastly, the white dot in Figure 8 is associated with a 1 minute t_p tolerance and a 4.2 revolution horizon time. This scenario is highlighted as an intermediate point between the lowest Δv case and the lowest perilune passage time case. This scenario results in the minimum standard deviation in this analysis. Table 2 lists the information highlighted by the green, red, and orange dots in Figure 8. The analysis of

different targeting parameters provides insight into the increase in maneuver cost to remain closer to the baseline trajectory. Additionally, perilune passage time serves as a proxy for the deviation between an as flown spacecraft and the baseline trajectory.

Table 1. Errors associated with stationkeeping simulation.

Error type	Error value
Insertion Position	2 km
Insertion Velocity	2 cm/s
Nav Position	1.5 km
Nav Velocity	0.8 cm/s
Maneuver Exection Direction	1°
Maneuver Exection Magnitude	1.5%
SRP Area	2%
SRP C_r	2%

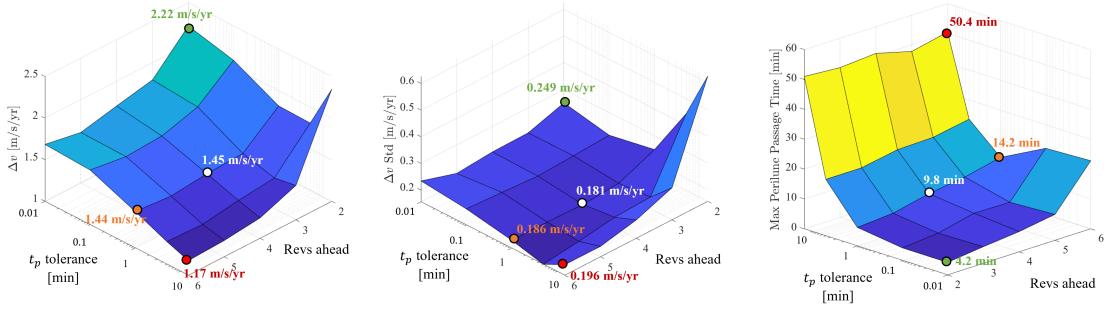

(a) (b) (c)

Figure 8. Results from Monte Carlo simulations using various combinations of horizon times and t_p tolerances. The (a) total OMM Δv per year, (b) total OMM Δv standard deviation, and (c) the maximum perilune passage time relative to the baseline NRHO. Note that the axes in the plot of (c) are rotated relative to (a) and (b).

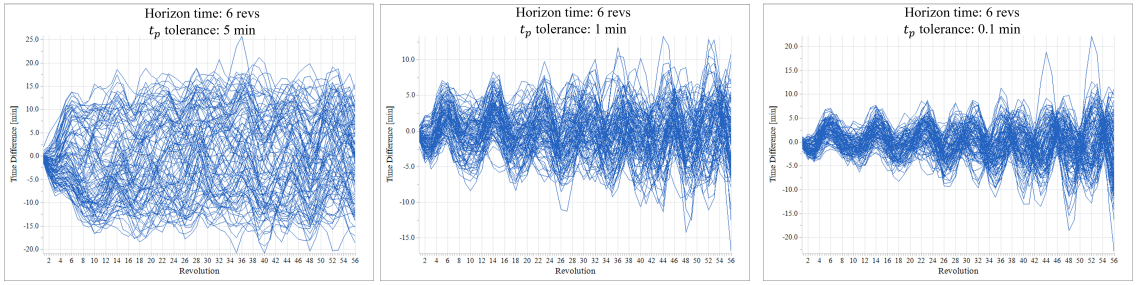

(a) (b) (c)

Figure 9. Perilune passage time for using a 6 rev horizon time with t_p tolerances of (a) 5 minutes, (b) 1 minute, and (c) 0.1 minutes.

The results displayed in Figure 8 are computed using a simplified simulation, where the Gateway is assumed to be a point mass, no attitude torques are modeled, and maneuvers are modeled as

Table 2. Highlighted lower-fidelity simulations from Figure 8 using the errors and perturbations in Table 1.

Horizon Time (revs ahead)	t_p Tolerance (min)	Δv (m/s/yr)	Δv Std (m/s/yr)	Max perilune passage time (min)	Max distance from baseline (km)
6	15	1.176	0.196	50.4	4895
6	1	1.44	0.186	14.2	1662
4	1	1.45	0.181	9.8	991.4
2	0.01	2.22	0.249	4.2	440.7

impulsive burns. To validate some of these results, a higher-fidelity simulation, called the Gateway Mission Design and Analysis Software (MiDAS), is leveraged.[29] A two-year mission for Gateway is simulated including events such as the docking of Orion, a human lander vehicle, and a logistics module. Additionally, the solar electric propulsion (SEP) system and chemical thrusters are modeled using finite burns for orbit maintenance maneuvers and desaturation maneuvers. Attitude torques are also numerically integrated using flat plate models for Gateway and visiting vehicles, and venting perturbations are modeled when applicable. For more details, see Newman et al.[29] First, a year-long simulation of an uncrewed Gateway is examined to understand the differences in Δv costs between the lower fidelity analysis summarized in Figures 8 and 9 and the higher-fidelity MiDAS simulation. Three scenarios are examined. The first uses the nominal OMM horizon time and t_p tolerance, i.e., 6 revolutions ahead and 15 minutes, the second scenario uses a horizon time of 4 revolutions ahead and 1 minute t_p tolerance, and the last scenario targets 2 revolutions ahead with a 0.01 minute t_p tolerance. The simulations are run with 100 Monte Carlo trials each, and the cumulative Δv and the perilune passage time variations are plotted in Figures 10(a) and 10(b). The statistics and results from the uncrewed MiDAS simulations are recorded in Table 3. Note that the maneuver costs are lower in the MiDAS simulation compared to the lower-fidelity simulations in Table 2. This difference indicates that the perturbations associated with the uncrewed, quiet Gateway configuration in the higher fidelity timeline are lower than for the generic Gateway model assumed in the lower fidelity simulation. Similarly, the vehicle adheres closer to the baseline NRHO trajectory in the MiDAS simulations in Figure 10 compared to the lower fidelity results in Table 2 since the disturbances on the spacecraft are smaller. These differences are due to the Gateway model selected for the MiDAS simulation, which represents the relatively small initial configuration of Gateway. As the Gateway stack size increases, OMM costs and variations also increase. However, the trends in Figure 10 follow the same pattern. With the longer horizon and the looser tolerance on t_p, the perilune passage time variations reach approximately 40 minutes after a year. In contrast, when the shorter 2-revolution horizon is employed with the 0.01 minute t_p tolerance, the perilune passage time remains within 3 minutes of the reference values over the year. However, as before, the tighter adherence to the baseline results in a higher orbit maintenance cost, with the annual Δv increasing from 0.49 m/s/yr to 1.57 m/s/yr with the tighter tolerances.

Table 3. MiDAS simulations for a year-long uncrewed Gateway mission.

Horizon Time (revs ahead)	t_p Tolerance (min)	Δv (m/s/yr)	Δv Std (m/s/yr)	Max perilune passage time (min)	Max distance from baseline (km)
6	15	0.49	0.073	50.4	4500
4	1	0.57	0.062	5.68	875
2	0.01	1.57	0.106	2.55	390

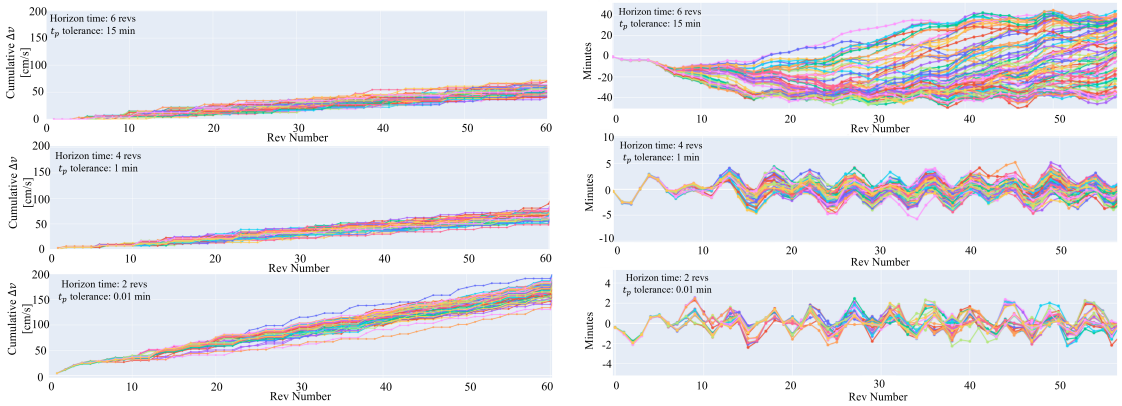

(a) (b)

Figure 10. MiDAS simulations of year-long, uncrewed Gateway missions. (a) Accumulated Δv costs over the simulation and (b) the perilune passage time relative to the NRHO baseline.

VARIATIONS BETWEEN AS-FLOWN SPACECRAFT

In the previous section, variations between a baseline trajectory and as-flown spacecraft are investigated. However, for vehicles loitering in the vicinity of Gateway, a comparison between as-flown Gateway and an as-flown loitering vehicle must be investigated as well. An understanding of the relative variations between as-flown vehicles provides insight into safe loitering in the NRHO. To characterize the variations, the OMM targeting horizon time and t_p tolerance are varied to assess how minimum separation distances between as-flown vehicles change when they adhere closer to their respective baseline trajectories.

Consider a scenario with the Gateway and a loitering vehicle operating in a string of pearls configuration. The Gateway is modeled in MiDAS as the uncrewed Power and Propulsion Element (PPE) and Habitation and Logistics Outpost (HALO) element. The loitering vehicle is modeled in the lower-fidelity orbit maintenance simulator, using impulsive burns and the errors and perturbations summarized in Table 1. While a wide variety of vehicles may loiter near Gateway with differing characteristics, the choice of the modeling characteristics is intended to give a conservative estimate of what is possible in the NRHO. Both vehicles are assumed to be performing OMMs using the Gateway orbit maintenance algorithm.[28] Vehicles loitering 1, 2, and 3 hours behind the Gateway are analyzed. First, both Gateway and the loitering vehicle at each of the three phases are considered using a horizon time of 6 revolutions ahead and t_p tolerance of 15 minutes. For each of the vehicles, 100 Monte Carlo trials are run and an all-to-all combination of the results appear in Figure 11. The top row of Figure 11 represents a vehicle loitering 1 hour behind the Gateway. In this case, the minimum separation distance in the dataset is 3 km, which represents insufficient margin for safe relative flight. The close proximity is also evidenced by the perilune passage time difference between Gateway and the loitering vehicle in Figure 11(b). Note how the difference crosses over the 0 hour mark, signifying that the loitering vehicle is no longer behind the Gateway. In the center row of Figure 11(b), the loitering vehicle located 2 hours behind Gateway has a minimum distance of approximately 230 km, but does not violate the 0 hour mark in the middle plot in Figure 11(b). Lastly, in the bottom row of Figure 11(b), the minimum separation between Gateway and a vehicle loitering 3 hours behind Gateway is 585 km, which is nearly double the minimum separation for

the -2 hour case. For all cases, the minimum separation occurs near apolune where relative speed is the slowest. These metrics provide insight into how close vehicles can safely be phased in a string of pearls when using the nominal Gateway OMM strategy. Comparing the minimum distance and the difference in perilune passage time also validates using perilune passage time difference as a proxy for close approach in string of pearls configuration. Since the NRHO in the CR3BP is symmetric and nearly symmetric in the ephemeris model, the results for phasing behind in Figure 11 are applicable to loitering ahead of the Gateway as well.

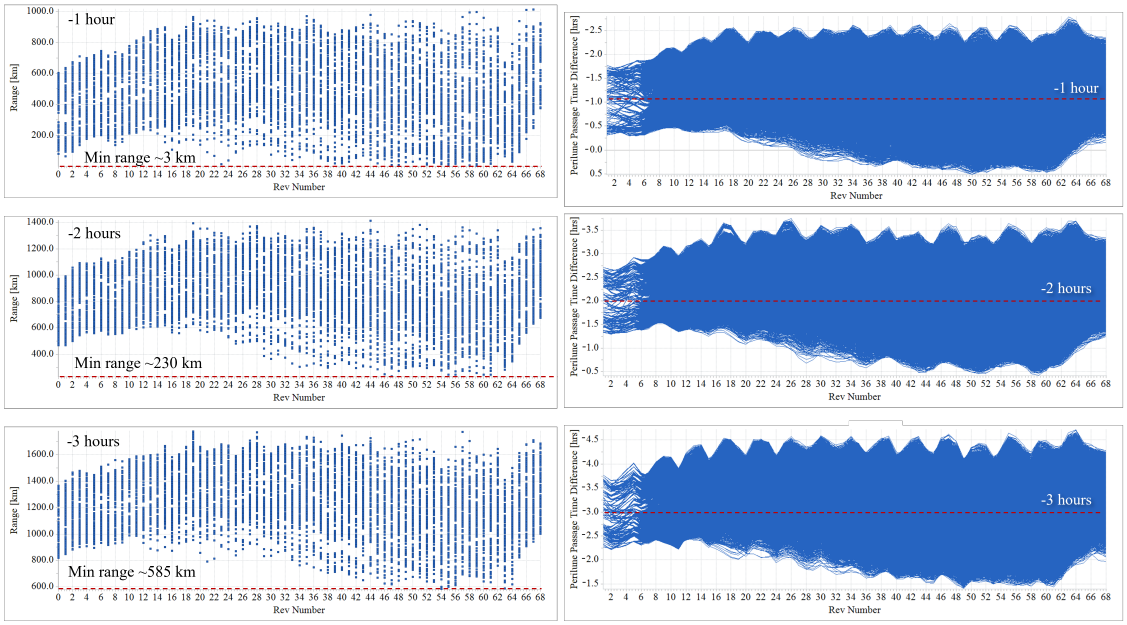

(a) (b)

Figure 11. (a) Minimum distance and (b) perilune passage time difference comparisions between Gateway and three loitering vehicles phased 1, 2, and 3 hours behind Gateway with a targeting horizon of 6 revolutions and a t_p tolerance of 15 minutes.

As demonstrated in a previous section, the targeting horizon time and t_p tolerance can be adjusted to adhere closer to a baseline NRHO. This strategy is applied to the Gateway and loitering vehicles to increase the separation distance between the vehicles. The horizon time and t_p tolerance are reduced to 2 revolutions ahead and 0.01 minutes, respectively, for each vehicle. Again, 100 Monte Carlo trials are run for spacecraft loitering 1, 2, and 3 hours behind Gateway, and an all-to-all comparison is completed. The minimum distance per revolution and the perilune passage time difference for all combinations of trials are plotted in Figure 12. In the scenario where the loitering vehicle is phased 1 hour behind, as plotted in the upper row of Figure 12, the minimum separation distance is now approximately 309 km, as compared to the 3 km using the nominal targeting parameters. Also note that each loitering vehicle remains much closer to its desired phasing with respect to Gateway in all three scenarios. Similarly, the minimum distance experienced by a spacecraft loitering 2 hours behind gateway increases to 687 km, as in the center row of Figure 12, and two spacecraft loitering 3 hours apart never come within 1066 km of each other, as in the lower row of Figure 12. By adhering closer to the baselines, the phasing 1 hour ahead or behind becomes a more viable option for a loitering phase since the risk of collision is reduced significantly. Referring to the analysis performed in the CR3BP shown in Figure 1, the minimum distance for 1 hour phasing is 374 km in

the CR3BP, which is similar to the minimum distance using the tighter orbit maintenance tolerances for as-flown vehicles in the ephemeris model. Additionally, it has been demonstrated by McCarthy et al. that transfer costs increase as the phasing time increases between vehicles in a string of pearls configuration.[7] By adhering closer to a baseline, the propellant cost to transfer to and from Gateway to a vehicles respective loitering phase is reduced as well.

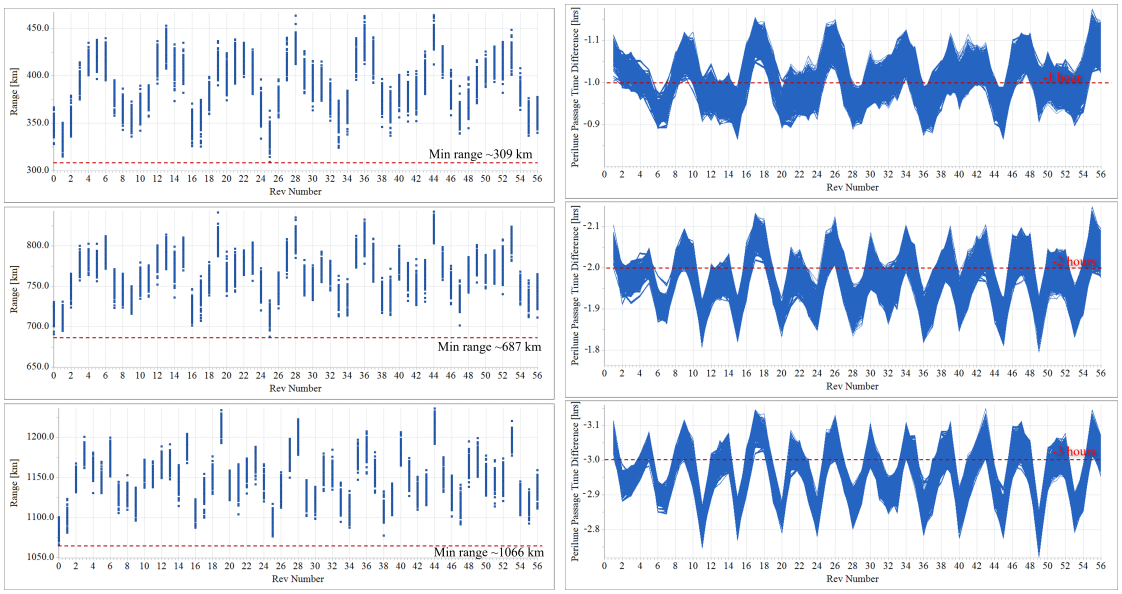

(a) (b)

Figure 12. (a) Minimum distance and (b) perilune passage time difference comparisons between Gateway and three loitering vehicles at 1, 2, and 3 hour phasing behind Gateway using a horizon time of 2 revs ahead and a t_p tolerance of 0.01 minutes.

CONCLUDING REMARKS

During the Artemis campaign, a significant number of visiting vehicles plan to visit the Gateway and loiter nearby. Therefore, analyzing various methods to loiter in the vicinity of the Gateway is critical to the success of the program. This investigation examines various aspects associated with loitering nearby. First, two configurations for loitering are examined, a string of pearls and a quasi-periodic orbit configuration. Trajectories associated with both configurations are constructed in a higher-fidelity ephemeris model. Unique characteristics associated with long-term NRHO baseline trajectories are examined and it is noted that the phasing drift needs to be considered when constructing baseline NRHOs phased ahead or behind the nominal phase. Quasi-periodic orbits possess unique characteristics that allow the loitering vehicle to "twist" or "spiral" around the Gateway NRHO. A parametric study on adjusting various stationkeeping parameters is conducted to understand the trade-off between remaining closer to the baseline NRHO and increased OMM costs. The results are validated in the higher-fidelity MiDAS simulation, which provides a more accurate representation of the operational Gateway. Lastly, comparisons are made between Gateway and three loitering vehicles in various string of pearls phasing locations. Using the technique of adjusting the OMM targeting parameters to remain closer to the NRHO baseline, the loitering vehicles remain closer to their respective baselines, reducing the possibility of a collision when loitering 1 hour behind the Gateway. This investigation does not address all aspects of safe loitering in the NRHO, but

it provides a first look at possible options and important considerations.

REFERENCES

[1] K. Hambleton, T. Fairley, and L. Cheshier, "Splashdown! NASA's Orion Returns to Earth After Historic Moon Mission," *web*, Dec. 2022.

[2] F. Khoury and K. Howell, "Orbital Rendezvous and Spacecraft Loitering in the Earth-Moon System," *AAS/AIAA Astrodynamics Specialist Conference*, Virtual, Aug. 2020.

[3] C. G. Sandel and R. Sood, "Low-Thrust Rendezvous and Proximity Operations in a Near Rectilinear Halo Orbit," *33rd AAS/AIAA Space Flight Mechanics Meeting*, Austin, Texas, Jan. 2023.

[4] D. C. Davis, E. M. Zimovan-Spreen, S. T. Scheuerle, and K. C. Howell, "Debris Avoidance and Phase Change Maneuvers in Near Rectilinear Halo Orbits," *44th Annual AAS Guidance, Navigation, and Control Conference*, Breckenridge, Colorado, Feb. 2022.

[5] E. Blazquez, L. Beauregard, S. Lizy-Destrez, F. Ankersen, and F. Capolupo, "Rendezvous design in a cislunar near rectilinear halo orbit," *Aeronautical Journal*, Vol. 124, Dec. 2020, pp. 821–837.

[6] G. Bucchioni, S. Lizy-Destrez, T. Vaujour, V. Thoraval, L. Rouverand, and C. Silva, "Phasing with near rectilinear Halo orbits: Design and comparison," Vol. 71, Mar., pp. 2449–2466.

[7] B. McCarthy, S. Scheuerle, E. Zimovan-Spreen, D. Williams, D. Davis, and K. Howell, "Rephasing and Loitering Strategies in the Gateway Near Rectilinear Halo Orbit," *AAS/AIAA Astrodynamics Specialist Conference*, Big Sky, Montana, August 2023.

[8] L. Nugent, M. Bolliger, A. Héritier, D. Davis, and K. Howell, "Short-Term Loitering in the Vicinity of the Gateway Near Rectilinear Halo Orbit in the Circular Restricted Three-Body Problem," *Rocky Mountain AAS GNC Conference*.

[9] L. Nugent and K. Howell, "Relative Trajectory Design Methodologies Informed by Stretching and Restoring Directions," *AAS/AIAA Astrodynamics Specialist Conference*.

[10] E. Zimovan-Spreen, S. Scheuerle, B. McCarthy, D. Davis, and K. Howell, "Baseline Orbit Generation for Near Rectilinear Halo Orbits," *AAS/AIAA Astrodynamics Specialist Conference*, Big Sky, Montana, 2023.

[11] D. C. Davis, B. P. McCarthy, and E. M. Zimovan-Spreen, "Perturbations and Recovery in the Gateway Near Rectilinear Halo Orbit," *33rd AAS/AIAA Spaceflight Mechanics Meeting*.

[12] V. Szebehely, *The Theory of Orbits: The Restricted Problem of Three Bodies*. New York, New York: Academic Press, Inc, 1967.

[13] C. H. Acton, *Ancillary Data Services of NASA's Navigation and Ancillary Information Facility*, Jan. 1996. https://naif.jpl.nasa.gov/naif/.

[14] S. Scheuerle, B. McCarthy, E. M. Zimovan-Spreen, and D. Davis, "Relative Motion for Short-term Loitering in the Gateway NRHO," *AAS/AIAA Spaceflight Mechanics Meeting*, Kauai, Hawaii, Jan. 2025.

[15] M. Miller, T. Snyder, and R. Hill, "Rendezvous Techniques," Tech Report FDD-ORB-RNDZ-006, NASA Johnson Space Center, Houston, Texas, Oct. 1998.

[16] J. Goodman, "Far Field Rendzvous Profile Design," Tech. Rep. JSC-67087, NASA Johnson Space Center, Houston, Texas, May 2017.

[17] I. Elliot and N. Bosanac, "Describing relative motion near periodic orbits via local toroidal coordinates," Vol. 134, No. 19.

[18] G. Brown, B. McCarthy, L. Peterson, D. Henry, D. Scheeres, and D. Davis, "Dynamics of the 9:2 Near Rectilinear Halo Orbit in the Sun-Earth-Moon System: Staging, Phasing and Transport," *75th International Astronautical Congress*, Milan, Italy, Oct. 2024.

[19] D. Henry and D. J. Scheeres, "Impulsive Spacecraft Formation Control on Quasi-Periodic Orbits," *2022 American Control Conference*.

[20] B. Barden and K. C. Howell, "Fundamental Motions Near Collinear Libration Points and Their Transitions," *Journal of the Astronautical Sciences*, Vol. 46, Dec. 1998, pp. 361–378.

[21] M. Dominguez and K. Howell, "Preliminary Design Strategy for Long-Term Loitering Orbits in Cislunar Space," *AAS/AIAA Astrodynamics Specialist Conference*.

[22] B. P. McCarthy and K. C. Howell, "Leveraging Quasi-Periodic Orbits for Trajectory Design in Cislunar Space," *Astrodynamics*, Vol. 5, June 2021, pp. 139–165. Issue 2.

[23] B. Park and K. Howell, "Assessment of Dynamical Models for Transitioning from the Circular Restricted Three-Body Problem to an Ephemeris Model with Applications," Vol. 136, No. 6.

[24] E. M. Zimovan-Spreen, D. C. Davis, and B. P. McCarthy, "Modeling and Phasing Considerations for Near Rectilinear Halo Orbit Baselines," *AAS/AIAA Astrodynamics Specialist Conference*, Big Sky, Montana, Aug. 2024.

[25] D. Villegas-Pinto, N. Baresi, S. Locoche, and D. Hestroffer, "Resonant Quasi-Periodic Near-Rectilinear Halo Orbits in the Elliptic-Circular Earth-Moon-Sun Problem," Vol. 71, pp. 336–354.

[26] B. Park and K. Howell, "Characterizing Transition-Challenging Regions Leveraging the Elliptic Restricted Three-Body Problem: L_2 Halo Orbits," *AIAA SciTech Forum*.

[27] D. J. Scheeres, "The Restricted Hill Four-Body Probem with Applications to the Earth-Moon-Sun System," Vol. 70, pp. 75–98.

[28] D. C. Davis, S. T. Scheuerle, D. A. Williams, F. S. Miguel, E. M. Zimovan-Spreen, and K. C. Howell, "Orbit Maintenance Burn Details for Spacecraft in a Near Rectilinear Halo Orbit," *AAS/AIAA Astrodynamics Specialist Conference*.

[29] C. P. Newman, C. Ott, A. Aguilar, and D. C. Davis, "Navigation Performance Overview of Gateway During a Lunar Lander Mission," *AAS/AIAA Astrodynamics Specialist Conference*, Broomfield, Colorado, Aug. 2024.